Published in final edited form as:
J Mater Sci. 2015 March ; 50(6): 2616–2625. doi:10.1007/s10853-015-8842-2.

Laminar Tendon Composites with Enhanced Mechanical Properties

Kyle A. Alberti[a], **Jeong-Yun Sun**[b,c,d], **Widusha R. Illeperuma**[b,c], **Zhigang Suo**[b,c], and **Qiaobing Xu**[a,*]

[a]Department of Biomedical Engineering, Tufts University, 4 Colby Street, Medford, Massachusetts, 02155, USA

[b]School of Engineering and Applied Sciences, Harvard University, Cambridge, Massachusetts, 02138, USA

[c]Kavli Institute for Bionano Science and Technology, Harvard University, Cambridge MA, 02138, USA

[d]Department of Materials Science and Engineering, Seoul National University, Seoul, 151-744 Korea

Abstract

Purpose—A strong isotropic material that is both biocompatible and biodegradable is desired for many biomedical applications, including rotator cuff repair, tendon and ligament repair, vascular grafting, among others. Recently, we developed a technique, called “bioskiving” to create novel 2D and 3D constructs from decellularized tendon, using a combination of mechanical sectioning, and layered stacking and rolling. The unidirectionally aligned collagen nanofibers (derived from sections of decellularized tendon) offer good mechanical properties to the constructs compared with those fabricated from reconstituted collagen.

Methods—In this paper, we studied the effect that several variables have on the mechanical properties of structures fabricated from tendon slices, including crosslinking density and the orientation in which the fibers are stacked.

Results—We observed that following stacking and crosslinking, the strength of the constructs is significantly improved, with crosslinked sections having an ultimate tens ile strength over 20 times greater than non-crosslinked samples, and a modulus nearly 50 times higher. The mechanism of the mechanical failure mode of the tendon constructs with or without crosslinking was also investigated.

Conclusions—The strength and fiber organization, combined with the ability to introduce transversely isotropic mechanical properties makes the laminar tendon composites a biocompatiable material that may find future use in a number of biomedical and tissue engineering applications.

[*]Corresponding Author: Phone: (617) 627-4322, Fax: 617-627-3231, Qiaobing.Xu@Tufts.

Disclosure:
The authors declare that there are no conflicts of interest.

Keywords

biomaterials; tendon; collagen; mechanical properties

1. Introduction

Many biomedical applications that utilize scaffolds or structures for implantation require a material that can undergo substantial loading while also being biocompatible. For example, rotator cuff patches designed to repair the torn tendon require strengths of at least 230N [1] in order to provide mechanical augmentation and prevent suture pull through of the tendon, a common problem of current repair patches [2,3]. Tendon and ligament repair patches and devices must be able to withstand physiological loads upwards of 2000N in a tissue that has little to no self-repair capability [4,5] such as the anterior cruciate ligament. Similarly, blood vessel prostheses require high burst pressures capable of resisting natural physiological forces and specific moduli to match the native tissue's compliance. Currently there are a number of products that support these high burst pressures, however, many are comprised of synthetic materials that are not biodegradable [6,7].

Recently, we developed a technique, called "bioskiving" to create both flat and tubular scaffolds out of decellularized tendon [8–11]. The process entails decellularizing a tendon, cutting it into blocks, and then sectioning the blocks parallel to the collagen fibers using a cryomicrotome (Fig. 1A). This creates thin sheets of collagen fibers that can then be stacked in a variety of directions (Fig. 1B,C).

The benefit of bioskiving is that it does not require denaturation and reconstitution of the collagen, which maintains the native triple helical structure, as well as the proteoglycan content [12,13]. This proves useful for both retaining the collagen's mechanical strength as well as the biological activity for cell interaction. The unidirectionally aligned collagen nanofibers (derived from sections of decellularized tendon) could offer good mechanical properties to constructs, such as prosthetic grafts. Additionally, the fibers contain nanotopographic features which can provide contact guidance for oriented cell growth, a useful feature for the fabrication of prosthetic conduits for nerve regeneration [14].

We found that these tendon sections are mechanically stronger than reconstituted collagen, but weaker than the native tendon [10,15,16]. In a previous study [10], we demonstrated that chemical crosslinking using 1-Ethyl-3-[3-dimethylaminopropyl]carbodiimide hydrochloride (EDC) could significantly reinforce the mechanical strength of the tendon-derived constructs. In this paper, we thoroughly studied the mechanical properties of the laminar collagen constructs while altering several variables, including the crosslinking density, and the orientation the fibers are stacked in. Glutaraldehyde (GTA) was selected as the chemical crosslinker because it is used extensively in the biomedical field for crosslinking and preparing decellularized extracellular matrices for implantation in several FDA approved products [17–19]. The mechanism by which the mechanical failure of the tendon constructs occurs was also investigated. We found that the collagen fibers are slipping within the non-collagen matrix (NCM) and that crosslinking could prevent this slippage, increasing the

mechanical strength. We also observed an improved transverse isotropy of the material by reorienting the direction of the collagen fibrils in adjacent tendon sections.

2. Materials and Methods

2.1 Collagen Section Fabrication and Crosslinking

Collagen sections were fabricated as previously described [10]. Briefly, frozen bovine Achilles tendon is cut into blocks ~20×20×2mm and placed into a decellularization solution containing 1% w/v sodium dodecyl sulfate (SDS) (Sigma, St. Louis, MO), 1mM Tris HCl, 0.1mM EDTA (Tris-EDTA pH 7.4, Sigma) in phosphate buffered saline (PBS), on a shaker at 4°C for 48h with the solution being changed after 24h. Following that, the blocks are rinsed in deionized water (diH_2O) and placed back onto the shaker in diH_2O for an additional 24h to remove residual SDS. The blocks are then frozen and sectioned on a cryomicrotome (CM1950, Leica Microsystems, Buffalo Grove, IL) at 50μm thick. The sections are stacked on a polytetrafluoroethylene (PTFE) block with fibers orientated in various directions as described in each section. The stacked sections are then air dried overnight, rinsed three times with diH2O and left to dry overnight again. The stacked sections are then immersed in 5% glutaraldehyde (Sigma) in PBS for 30min unless otherwise indicated. The samples are then rinsed three times in PBS and air dried until later use.

2.2 ATR-FTIR Analysis

Analysis was conducted using an ATR-FTIR spectrophotometer (FT-IR 6000, Jasco, Easton, MD). Three samples each of 10-layer stacked sections, rinsed but non-crosslinked and 5% glutaraldehyde crosslinked samples were analyzed. The samples were scanned from 600cm^{-1} to 4000cm^{-1}.

2.3 Crosslinking Density Testing

Sections (50μm thick) were stacked in 10 layers with all fiber directions oriented parallel to each other. The sections were then crosslinked for 20 min at glutaraldehyde concentrations of 0.1%, 0.5%, 1% and 2.5%, or not crosslinked. Each sample was then glued between two acrylic plates using super glue, and tested under uniaxial tension at a strain rate of 2mm/min on a mechanical testing apparatus (Instron, Norwood, MA) with a 1000N load cell until failure.

2.4 Pulling-Angle Testing

Sections (50μm thick) were stacked in 10 layers with all fiber directions oriented parallel to each other. The sections were then crosslinked with 5% glutaraldehyde for 30min. Each stack was then tested in one of three orientations: fibers in line with the direction of the force ($\theta = 0°$), fibers oriented at an angle to the applied force ($\theta = 45°$), or with fibers perpendicular to the direction of applied force ($\theta = 90°$).

2.5 Stacking-Angle Testing

Sections (50μm thick) were stacked in 12 layers during fabrication with alternating fiber orientations. Following the first section, each subsequent section was rotated either: 0°, 30°, 45°, or 90°. This pattern was repeated until all 12 sections had been placed with the degree of rotation remaining constant within a single sample.

2.6 Scanning Electron Microscopy

Samples that had been tested until failure were removed from the tensile testing setup, air dried overnight, further dehydrated in graded ethanol and finally dried with hexamethyldisilazane (Sigma). The samples were then sputter-coated with Pt-Pd using a Cressington 208HR Sputter-coater (Cressington Scientific, Watford, Hertfordshire, UK) and imaged using a Zeiss Ultra-55 Scanning Electron Microscope (Zeiss, Oberkochen, Germany)

2.7 Mechanical and Statistical Analysis

Ultimate tensile strength (UTS) was determined as the maximum stress of each sample's stress-strain curve. The elastic modulus was calculated via linear regression of the slope of the stress-strain curve. All values reported as mean ± standard error and a sample size of n=4 was used for all conditions. Differences in UTS and modulus were analyzed by analysis of variance (ANOVA) with post hoc Tukey's testing using IBM SPSS software (IBM, Armonk, NY).

3. Results

3.1 ATR-FTIR Analysis of the GTA crosslinked tendon constructs

Tendon samples were crosslinked via glutaraldehyde reaction where the primary mechanism is the formation of Schiff base intermediates between amine groups, primarily of lysine and hydroxylysine residues (Fig. 2A). Non-crosslinked samples analyzed by attenuated total reflectance – Fourier transform infrared (ATR-FTIR) (Fig. 2B) spectroscopy exhibited typical peaks associated with collagen for amide I, amide II and amide III at 1636cm^{-1}, 1536cm^{-1} 1230cm^{-1} respectively, as well as peaks associated with secondary amines (3260cm^{-1}), methylene bridges (2915 and 2850cm^{-1}) and imines (1700cm^{-1}). Tendon crosslinked with GTA showed similar peaks however the ratio of both secondary amines to methylene bridges (1:0.58 (NC) compared to 1:0.87 (GTA)) and secondary amines to imines (1:0.48 (NC) compared to 1:0.51(GTA)) changed.

3.2 Mechanical strength testing of constructs with various crosslinking densities

Tensile testing resulted in a difference in mechanical properties between crosslinked and non-crosslinked samples however as the crosslinking density increases the mechanical properties level off (Fig. 3). Non-crosslinked (0%) samples had a UTS of 0.63 ±0.07MPa and a modulus of 3.11 ±1.35MPa, while 0.1% crosslinked samples had a UTS of 4.55 ±0.34MPa and a modulus of 48.17±3.58MPa, 0.5% crosslinked samples a UTS of 11.25±1.35MPa and modulus of 95.86±16.1MPa, 1% a UTS of 13.32 ±0.643MPa and a modulus of 129.08±10.44MPa, and 2.5% a UTS of 13.59±1.35MPa and a modulus of

145.54 ±18.72MPa. Non-crosslinked samples appeared to have fibers slide apart in the midsection (Fig. 3D,E) while crosslinked samples appeared to have small cracks propagate from the initial failure points (Fig. 3F,G).

3.3 Scanning Electron Microscopy

SEM images of non-crosslinked samples and crosslinked samples appeared to have different methods of failure. The non-crosslinked samples (Fig. 4A) have a smooth edge which shows that adjacent fibers may have pulled apart from each other, and curled back at the micro-scale (Fig. 4C inset), leaving a smooth edge at the larger scale (Fig. 4C). The crosslinked sample (Fig. 4B) however appears to have a rough edge (Fig. 4D) where the fracture propagated, with abruptly ending fibers at the micro-scale (Fig. 4D inset).

3.4 Pulling-Angle Testing

In order to verify and the anisotropic mechanical nature of the tendon due to the collagen fibers we tested crosslinked samples comprised of aligned collagen fibers where the direction of applied force was at an angle to the fiber orientation (Fig. 5a). Application of force in the direction of the fibers (0°) yielded the highest UTS with 10.84 ± 1.25MPa, while force applied at 45° and 0° resulted in UTS of 3.90 ± 0.47MPa and 1.17 ± 0.21 MPa. Similar results were seen with the moduli, where the samples tested at 0° had a modulus of 158.29 ± 21.11 MPa, 45° a modulus of 41.72 ± 8.83 MPa and 90° a modulus of 15.48 ± 5.28 MPa (Fig. 5).

3.5 Stacking-Angle Testing

Stacking sections of tendon at various orientations has the goal of creating a transverse isotropic material. Sections rotated by 0°, 30°, 45° and 90° (Fig. 6A,B) for each section and crosslinked, should have different mechanical properties. Samples where all the fibers were aligned (0°) had a UTS of 10.84 ± 1.25MPa and a modulus of 158.29 ± 21.11MPa, 30° rotation a UTS of 6.34 ± 0.93 MPa and modulus of 81.71 ± 13.1 MPa, 45° rotation a UTS of 8.25 ± 0.78 MPa (Fig. 6C) and modulus of 108.77 ± 10.6 MPa, and 90° rotation a UTS of 4.71 ± 0.59 MPa and modulus of 74.03 ± 16.21 MPa (Fig. 6C,D).

4. Discussion

4.1 Fabrication of tendon-derived sections

Following the bioskiving process, we are able to generate two dimensional and three dimensional constructs. This process utilizes tendon as the source material, however it could be used with other decellularized biological tissues. Tendon was used as it comprises highly aligned collagen fibers at several length scales, which give the native material very strong mechanical properties, upwards of 125MPa ultimate tensile strength [12,20,22]. Previously we reported on the bioskiving process to produce structures with 90° fiber orientations for applications such as tissue engineered blood vessels, where the desired outcome was a compliant material (low modulus). Even though the mechanical strength of the collagen constructs derived from tendon slices are stronger than that from reconstituted collagen, these sectioned materials were surprisingly weaker compared to the native tendon, and to reports of materials processed in a similar manner [21]. In an attempt to improve the

observed mechanical properties we crosslinked the material with EDC as it is more biocompatible than several other chemical crosslinkers. This produced only a slight improvement to the material's strength, and did not restore it to pre-processing strength.

Here, we attempt to re-engineer the tendon-derived constructs with robust mechanical properties that would be better suited for biomedical applications that require high strength. Thinking along these lines, we decided to use GTA as a crosslinker, as it crosslinks via the addition of a linker arm between amines [23] (Fig. 2A), and could therefore crosslink collagen fibers that have more distance between them. Additionally, previous experiments have shown greater mechanical properties with GTA than EDC [24,25], and GTA is commonly used for a number of biomedical applications [17]. It is noted however, that GTA can have cytocompatibility and host response issues [26,27], however we believe the increased mechanical strength and longer degradation rate [28] are of greater benefit. Therefore, in this paper, GTA was used at varying concentrations. To confirm that GTA-mediated crosslinks were actually forming, crosslinked and non-crosslinked tendon sections were observed via ATR-FTIR (Fig. 2B). Non-crosslinked tendon samples displayed peaks at wavenumbers characteristic of tendon [29] (ex. amide peaks at 1630–1635cm^{-1}) and once crosslinked, the expected peaks developed [30,31]. These include a decrease in the ratio of secondary amines at 3260cm^{-1} to imines at 1700cm^{-1} and methylene bridges at 2915cm^{-1} and 2850cm^{-1}, associated with the formation of a carbon-nitrogen double bond between the GTA and an amine of the collagen molecules, and the addition of the methylene bridge of the GTA, respectively. Additionally, when the collagen blocks are crosslinked prior to being sectioned and stacked, the sections will not adhere to each other during the drying process. This observation indicates that the pre-crosslinking depletes the reactive groups in the tendon which prevents adhesion between layers through hydrogen-bonding.

4.2 Failure mode of tendon-derived sections

Fig. 3A–C shows the mechanical properties of the non-crosslinked tendon sections (0% GTA), similar to those observed previously for samples with aligned fibers (<1MPa UTS, <5MPa modulus). Native tendon has much greater mechanical strength than this due to its hierarchical structure and fibril-fascicle-tendon structure that prevents the failure of the non-continuous uniform fibers from early failure. We hypothesize that the sectioning process disrupts this macro-fascicular strengthening as discussed previously [15], and the decellularization may disrupt the proteoglycans that make up the NCM, and the crosslinks between the collagen fibrils and the NCM. This allows fracture between the fibers and the matrix, resulting in the failure. Crosslinking with GTA should re-introduce crosslinks between the proteoglycans and the collagen, as well as inter-collagen crosslinks. A macroscopic view of the non-crosslinked sample failure can be seen in Fig. 3D,E where large portions of the tendon-sections pull apart, with multiple locations appearing to have multiple failure points along the direction of applied force. As expected, crosslinking with GTA increases the mechanical strength, proportional to the amount of crosslinker, until the samples are saturated and maximally crosslinked. Fig. 3F,G shows the macroscopic failure of maximally-crosslinked samples, where the failure appears to be a complete transverse fracture across the width of the sample.

To confirm this observation at the micro-scale, sections were imaged before and after failure with a scanning electron microscope. Prior to testing, both non-crosslinked and crosslinked appear to be identical (Fig. 4), being primarily comprised of large sections of continuous, highly aligned collagen fibrils. However, after testing, the failure point of the non-crosslinked sections appears to be relatively smooth, while the failure point of the crosslinked sections is abrupt and jagged. This dissimilarity is a result of differences in the failure mechanism before and after crosslinking. In the non-crosslinked samples, many of the crosslinks between the fibers and matrix have been disrupted, which allows for the sliding of the collagen fibrils past each other, as the fibrils are relatively short (5–20 mm [32,33]). This type of failure can be compared to the shear-lag model for failure of short-fibered composites developed by Cox [34], explaining failure by delamination and fiber pull-out [35–37], where stress is transferred from the matrix to the fibers by interfacial shear stress. However, with the reduction in the number of crosslinks between the NCM and the fibrils, the fibrils slip past each other slowly at much lower stresses, resulting in the ends of various fibers creating a relatively smooth edge. This is not observed in native tendon, as the bundled tendon fascicles are believed to extend the length of the tendon [38] and could be considered ‘continuous’, however do to their short length, collagen fibrils do not [32,39].

In the crosslinked samples, the interfacial shear stresses are much greater. At the point where the interfacial shear stresses exceed the tensile strength of the fibrils in the material, the mode of failure changes. The new failure method is rapid fracture of collagen fibrils at various points, resulting in the jagged appearance of the fiber ends. More magnified examination of both samples make the failure more clear, where there are curled fibrils at the end of one ‘bundle’ of collagen fibrils on the non-crosslinked sample (Fig. 4C inset), and a distinct edge at the edge of the end of a bundle of collagen fibrils in the crosslinked sample where the fracture propagated (Fig. 4D inset).

4.3 Fiber alignment and enhanced mechanical properties

The stacked sections show improved mechanical properties following crosslinking, however that is only when force is applied in the direction of the fibers. When force is applied in another direction, such as 45° or 90° to the fibers as shown in Fig. 5 the ultimate tensile strength is greatly reduced as is the modulus. This is as expected as the force is no longer being applied to the fibers themselves, but rather the strength is dependent on the matrix. A similar phenomenon is seen in many anisotropic materials, and one method to produce improved isotropic strength is to create laminar composite where the fiber orientation is rotated in adjacent sheets. Perhaps the most common example of this is the multilayer construction of plywood; however this technique is also used widely in the construction of other organic or metallic-fiber based materials [40]. Similar arrangements of varying fiber orientations can also be found in nature, such as is present in the remarkably tough scales of the Arapaima fish, which contain a twisting arrangement of collagen fibril lamellae[41].

This laminar composite technique was also used with the tendon derived sheets, alternating the ply orientation by either: 0°, 30°, 45° or 90° (Fig. 6) in an effort to create a transversely isotropic material. Following stacking of the sections, the mechanical strength of each material was evaluated under uniaxial tension. While the material’s strength was only

evaluated in the primary direction, each direction of fiber orientation should have the same properties. The samples with no fiber rotation were expected to have the greatest mechanical strength as they contain 12 layers in the primary direction whereas the other sections have either 3 sections in each orientation (30° rotation), 4 sections (45° rotation) or 6 sections (90° rotation). However, even with fewer sections in the direction of applied force, the 45° rotated samples were not statistically weaker than the 0° sections (Fig. 4C), nor was the material any less elastic (Fig. 4D). Interestingly, the 90° rotated sections were significantly weaker, despite a greater number of sections. Therefore, a 45° rotation of fiber orientation should be the optimal strategy for fabricating transversely isotropic materials from tendon-derived sections. One could also imagine that increasing the section thickness would provide this mechanical strength without the need for crosslinking; however, these thin sections are useful as substrates for cell-seeding. Additionally, thick sections would still have the problem of anisotropic mechanical properties, and the fabrication of a laminar composite would be limited, as individual laminate thicknesses must remain small compared to other material dimensions [40,42].

5. Conclusions

There exists a need for a strong biomaterial that is biodegradable and biocompatible, with isotropic mechanical properties. The bioskiving process can be used to produce laminate composites from thin sections of decellularized tendon. Crosslinking these composites greatly improves their mechanical strength over non-crosslinked samples, increasing the ultimate tensile strength over 20 fold to a maximum strength of 13.59MPa, and increasing the modulus nearly 50 fold to 145.54. Rotating adjacent layers of the stacked sections also enables the enhancement of transversely isotropic mechanical properties as the native collagen material is strong in the direction of fiber orientation but weak perpendicularly to that. Overall, constructs fabricated from tendon-derived collagen have good isotropic strength and the potential to be used for numerous biomedical applications.

Supplementary Material

Refer to Web version on PubMed Central for supplementary material.

Acknowledgements

QX acknowledges Pew Scholar for Biomedical Sciences program from Pew Charitable Trusts and NIH (1R03EB017402-01). KA acknowledges the IGERT fellowship from NSF. This work utilized the facilities at the Harvard University Center for Nanoscale Systems (CNS), a member of the National Nanotechnology Infrastructure Network (NNIN), which is supported by the National Science Foundation under NSF award no. ECS-0335765. We would also like to thank Todd Fritz for the photographs of the tendon sections in Fig. 1.

References

1. Derwin KA, Badylak SF, Steinmann SP, Iannotti JP. Extracellular matrix scaffold devices for rotator cuff repair. J. Shoulder Elbow Surg. 2010; 19:467–476. [PubMed: 20189415]
2. Aurora A, McCarron J, Iannotti JP, Derwin K. Commercially available extracellular matrix materials for rotator cuff repairs: state of the art and future trends. J. Shoulder Elbow Surg. 2007; 16:S171–S178. [PubMed: 17560804]

3. Coons DA, Barber AF. Tendon graft substitutes-rotator cuff patches. Sports Med. Arthrosc. 2006; 14:185–190. [PubMed: 17135966]
4. Altman GH, Horan RL, Lu HH, Moreau J, Martin I, Richmond JC, Kaplan DL. Silk matrix for tissue engineered anterior cruciate ligaments. Biomaterials. 2002; 23:4131–4141. [PubMed: 12182315]
5. Altman GH, Diaz F, Jakuba C, Calabro T, Horan RL, Chen J, Lu H, Richmond J, Kaplan DL. Silk-based biomaterials. Biomaterials. 2003; 24:401–416. [PubMed: 12423595]
6. Xu W, Zhou F, Ouyang C, Ye W, Yao M, Xu B. Mechanical properties of small-diameter polyurethane vascular grafts reinforced by weft-knitted tubular fabric. J Biomed Mater Res A. 2010; 92:1–8. [PubMed: 19165779]
7. Dahl SLM, Rhim C, Song YC, Niklason LE. Mechanical properties and compositions of tissue engineered and native arteries. Ann Biomed Eng. 2007; 35:348–355. [PubMed: 17206488]
8. Dai X, Xu Q. Nanostructured substrate fabricated by sectioning tendon using a microtome for tissue engineering. Nanotechnology. 2011; 22:494008. [PubMed: 22101489]
9. Dai X, Schalek R, Xu Q. Staining and Etching: A Simple Method to Fabricate Inorganic Nanostructures from Tissue Slices. Adv Mater. 2011; 24:370–374. [PubMed: 22174186]
10. Alberti KA, Xu Q. Slicing, Stacking and Rolling: Fabrication of Nanostructured Collagen Constructs from Tendon Sections. Adv Healthc Mater. 2013; 2:817–821. [PubMed: 23233344]
11. Alberti, KA.; Xu, Q. Bioinspired Fabrication of Nanostructures from Tissue Slices. In: Jabarri, E., editor. Handbook of Biomimetics and Bioinspiration: Biologically-Driven Engineering of Materials, Processes, Devices and Systems. Singapore: World Scientific Publishing Company; 2014.
12. Ning LJ, Zhang Y, Chen XH, Luo JC, Li XQ, Yang ZM, Qin TW. Preparation and characterization of decellularized tendon slices for tendon tissue engineering. J Biomed Mater Res A. 2012; 100:1448–1456. [PubMed: 22378703]
13. Cartmell JS, Dunn MG. Development of cell-seeded patellar tendon allografts for anterior cruciate ligament reconstruction. Tissue Eng. 2004; 10:1065–1075. [PubMed: 15363164]
14. Alberti KA, Hopkins AM, Tang-Schomer MD, Kaplan DL, Xu Q. The behavior of neuronal cells on tendon-derived collagen sheets as potential substrates for nerve regeneration. Biomaterials. 2014; 35:3551–3557. [PubMed: 24461939]
15. Qin TW, Chen Q, Sun YL, Steinmann SP, Amadio PC, An KN, Zhao C. Mechanical characteristics of native tendon slices for tissue engineering scaffold. J Biomed Mater Res B Appl Biomater. 2012; 100:752–758. [PubMed: 22323314]
16. Cartmell J, Dunn M. Effect of chemical treatments on tendon cellularity and mechanical properties. J. Biomed. Mater. Res. 2000; 49:134–140. [PubMed: 10559756]
17. Jayakrishnan A, Jameela SR. Glutaraldehyde as a fixative in bioprostheses and drug delivery matrices. Biomaterials. 1996; 17:471–484. [PubMed: 8991478]
18. Dahl SLM, Kypson AP, Lawson JH, Blum JL, Strader JT, Li Y, Manson RJ, Tente WE, DiBernardo L, Hensley MT, Carter R, Williams TP, Prichard HL, Dey MS, Begelman KG, Niklason LE. Readily available tissue-engineered vascular grafts. Sci Transl Med. 2011; 3:68ra9.
19. Kehoe S, Zhang XF, Boyd D. FDA approved guidance conduits and wraps for peripheral nerve injury: A review of materials and efficacy. Injury. 2011; 43:553–572. [PubMed: 21269624]
20. Yamamoto N, Hayashi K, Kuriyama H, Ohno K, Yasuda K, Kaneda K. Mechanical properties of the rabbit patellar tendon. J Biomech Eng. 1992; 114:332–337. [PubMed: 1522727]
21. Wren TA, Yerby SA, Beaupré GS, Carter DR. Mechanical properties of the human achilles tendon. Clin. Biomech. (Bristol, Avon). 2001; 16:245–251.
22. Johnson GA, Tramaglini DM, Levine RE, Ohno K, Choi NY, Woo SL. Tensile and viscoelastic properties of human patellar tendon. J Orthop Res. 1994; 12:796–803. [PubMed: 7983555]
23. Cheung DT, Perelman N, Ko EC, Nimni ME. Mechanism of crosslinking of proteins by glutaraldehyde III. Reaction with collagen in tissues. Connect Tissue Res. 1985; 13:109–115. [PubMed: 3157539]
24. Ber S, Torun Köse G, Hasirci V. Bone tissue engineering on patterned collagen films: an in vitro study. Biomaterials. 2005; 26:1977–1986. [PubMed: 15576172]

25. Barnes CP, Pemble CW, Brand DD, Simpson DG, Bowlin GL. Cross-linking electrospun type II collagen tissue engineering scaffolds with carbodiimide in ethanol. Tissue Eng. 2007; 13:1593–1605. [PubMed: 17523878]
26. Brown BN, Barnes CA, Kasick RT, Michel R, Gilbert TW, Beer-Stolz D, Castner DG, Ratner BD, Badylak SF. Surface characterization of extracellular matrix scaffolds. Biomaterials. 2010; 31:428–437. [PubMed: 19828192]
27. Dahm M, Lyman WD, Schwell AB, Factor SM, Frater RW. Immunogenicity of glutaraldehyde-tanned bovine pericardium. J Thorac Cardiovasc Surg. 1990; 99:1082–1090. [PubMed: 2141662]
28. Liang HC, Chang Y, Hsu CK, Lee MH, Sung HW. Effects of crosslinking degree of an acellular biological tissue on its tissue regeneration pattern. Biomaterials. 2004; 25:3541–3552. [PubMed: 15020128]
29. Vidal BDC, Mello MLS. Collagen type I amide I band infrared spectroscopy. Micron. 2011; 42:283–289. [PubMed: 21134761]
30. Wang X, Zhang J, Wang Q. Surface Modification of GTA Crosslinked Collagen-based Composite Scaffolds with Low Temperature Plasma Technology. J Macromol Sci Part A. 2008; 45:585–589.
31. Ocak B. Complex coacervation of collagen hydrolysate extracted from leather solid wastes and chitosan for controlled release of lavender oil. J Environ Manage. 2012; 100:22–28. [PubMed: 22361107]
32. Legerlotz K, Riley GP, Screen HRC. Specimen dimensions influence the measurement of material properties in tendon fascicles. J Biomech. 2010; 43:2274–2280. [PubMed: 20483410]
33. Buehler MJ. Multiscale Mechanics of Biological and Biologically Inspired Materials and Structures. Acta Mech Solida Sinica. 2010; 23:471–483.
34. Cox H. The elasticity and strength of paper and other fibrous materials. Br J Appl Phys. 1952; 3:72.
35. Drzal LT, Madhukar M. Fibre-matrix adhesion and its relationship to composite mechanical properties. J Mater Sci. 1993; 28:569–610.
36. Garett KW, Bailey JE. Multiple transverse fracture in 90 cross-ply laminates of a glass fiber-reinforced polyester. J Mater Sci. 1977; 12:157–168.
37. Aveston J, Kelly A. Theory of multiple fracture of fibrous composites. J Mater Sci. 1973; 8:352–362.
38. Amis AA, Basso O, Johnson DP. The anatomy of the patellar tendon. Knee Surgery, Sport Traumatol Arthrosc. 2001; 9:2–5.
39. Provenzano PP, Vanderby R. Collagen fibril morphology and organization: implications for force transmission in ligament and tendon. Matrix Biol. 2006; 25:71–84. [PubMed: 16271455]
40. Vinson, JR.; Sierakowski, RL. The Behavior of Structures Composed of Composite Materials. The Netherlands: Springer; 2006.
41. Zimmermann EA, Gludovatz B, Schaible E, Dave NKN, Yang W, Meyers MA, Ritchie RO. Mechanical adaptability of the Bouligand-type structure in natural dermal armour. Nat Commun. 2013; 4:1–7.
42. Staab, G. Laminar Composites. Oxford: Butterworth-Heinemann; 1999.

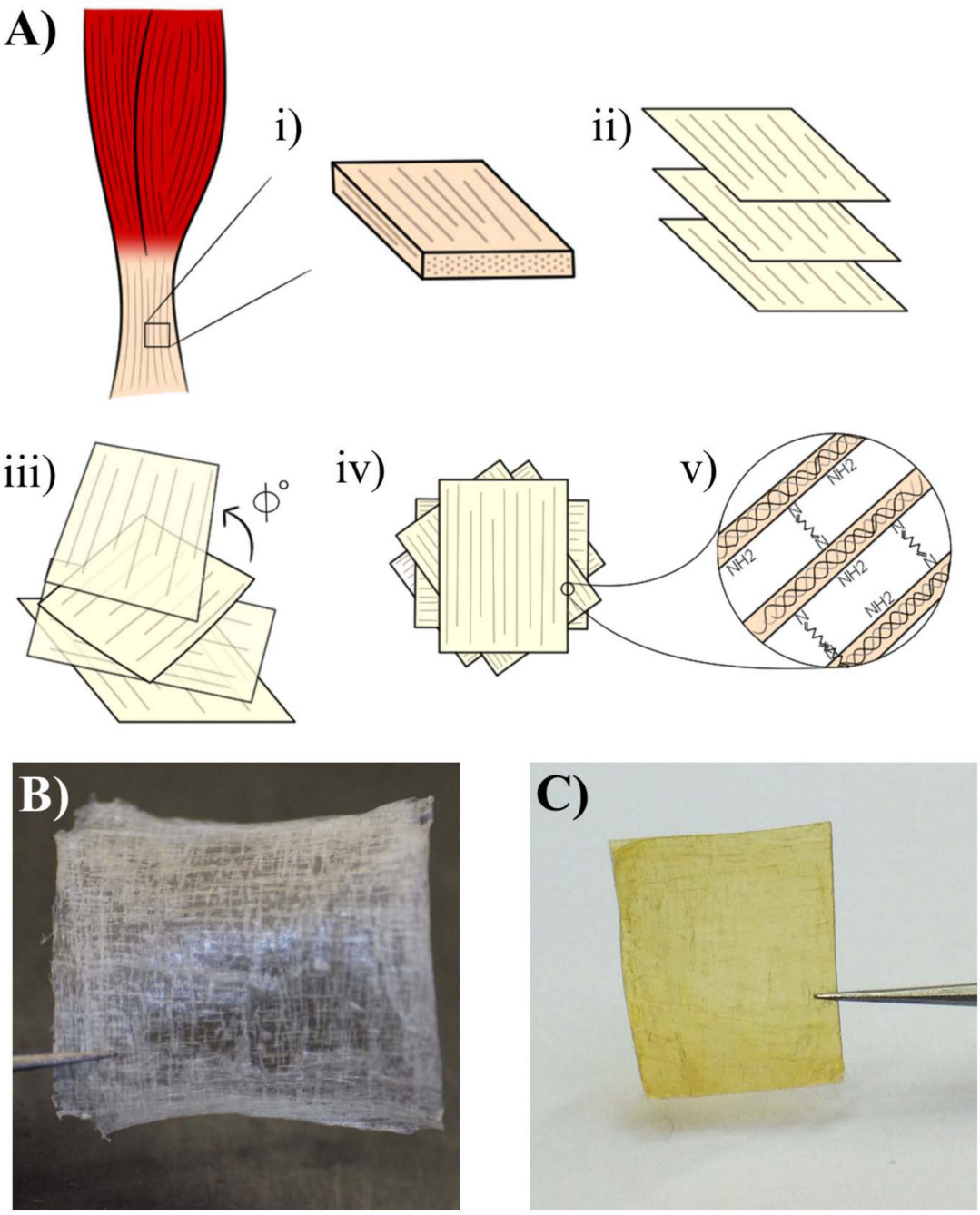

Fig. 1.

A) Schematic illustrating the bioskiving process involving: i. cutting a block (~20×20×2mm) from a piece of tendon; ii. decellularizing the block, and sectioning it into thin sections; iii. stacking the sections with fibers in various orientations (each rotated by Φ degrees); iv. drying and washing the sections; v. crosslinking the sections (e.g. glutaraldehyde). **B)** Photograph of non-crosslinked tendon sections. 10 layers of 50μm thick sections were stacked, and each layer has 90° rotation to the adjacent layer. **C)** Photograph

of crosslinked tendon sections. Tendon sections which have the same geometry as (B) were crosslinked with glutaraldehyde

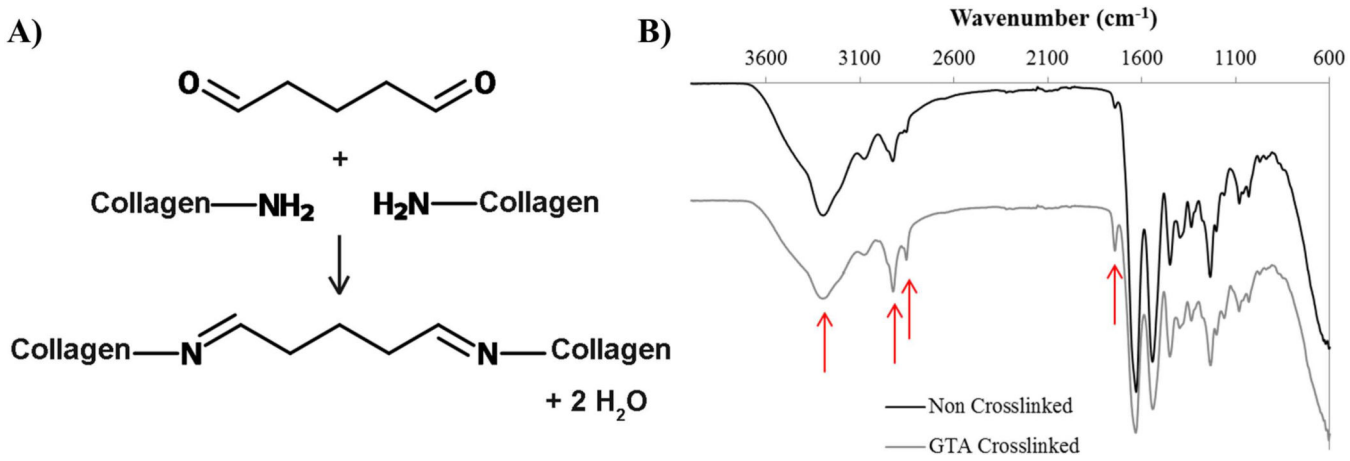

Fig. 2.

A) Illustration of a simplified mechanism of GTA crosslinking mechanism in collagen **B)** FTIR spectrum of non-crosslinked and glutaraldehyde crosslinked tendon samples. Arrows from left to right in both graphs are 3260cm^{-1} (secondary amine), 2915cm^{-1} and 2850cm^{-1} (methylene bridge), and 1700cm^{-1} (imine). From non-crosslinked to crosslinked the ratio of secondary amines to imine and methylene decreases showing the crosslinking of the secondary amines with glutaraldehyde

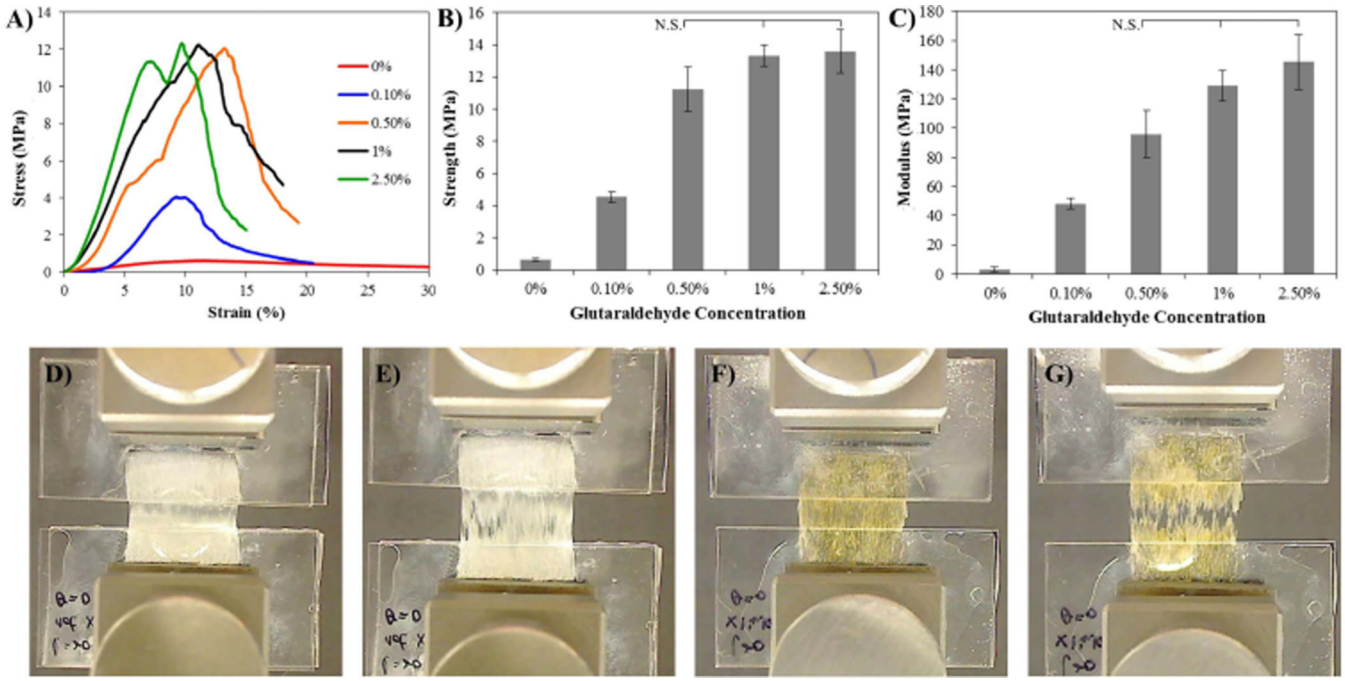

Fig. 3.

A) Representative stress strain curves of 10-layer (50μm thick each) stacked samples that have been crosslinked with various concentrations of glutaraldehyde (0.1, 0.5, 1, 2.5%) for 20 min., or not crosslinked (0%). **B, C)** Graphs illustrating the ultimate tensile strength and elastic modulus, respectively, of crosslinked samples. **D)** Photographs showing uniaxial tensile testing of non-crosslinked samples prior to testing and **E)** at failure. **F)** Photographs showing uniaxial tensile testing of 2.5% glutaraldehyde-crosslinked samples prior to testing and **G)** at failure. Stress and modulus that are not statistically different are marked N.S.; all other comparisons have $p>0.05$, ($n=4$) for all samples. Native rat tendon has been shown to have a UTS of 64.1 ± 3.87 MPa and a modulus of 632 ± 51.3 MPa [16]. Strength and moduli values are given in Supplementary Fig. 1

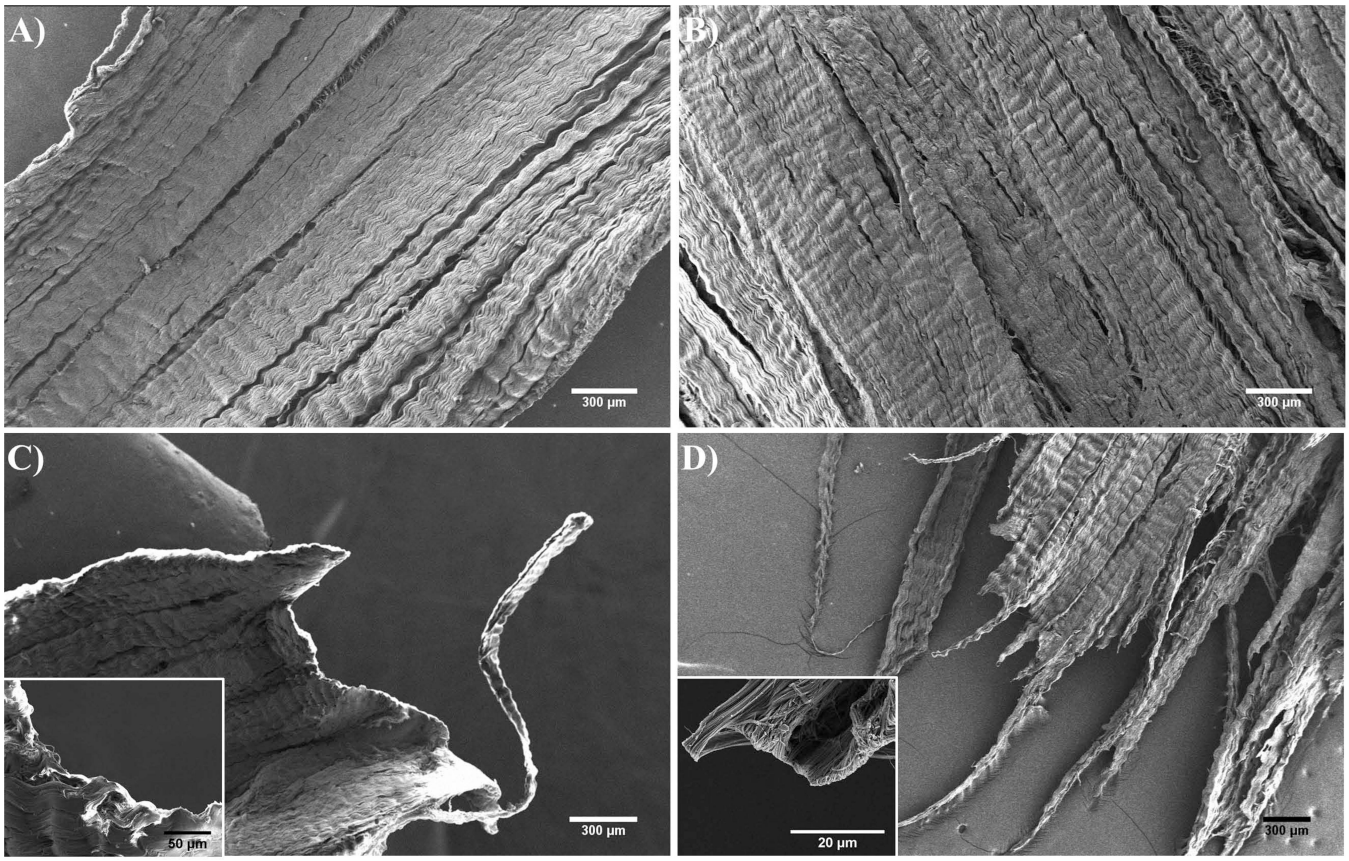

Fig. 4.

A,B) Scanning electron micrographs of a section of non-crosslinked, and glutaraldehyde crosslinked tendon-stacks prior to testing, respectively. **C,D)** Scanning electron micrographs of a section of non-crosslinked and glutaraldehyde-crosslinked (5%, 30min) tendon-stacks prior to testing, and the failure-point following rupture under tension. All samples consist of 10 layers with a thickness of 50µm for each layer. All layers have their fiber orientations aligned in the same direction and were tested with the force applied in that direction

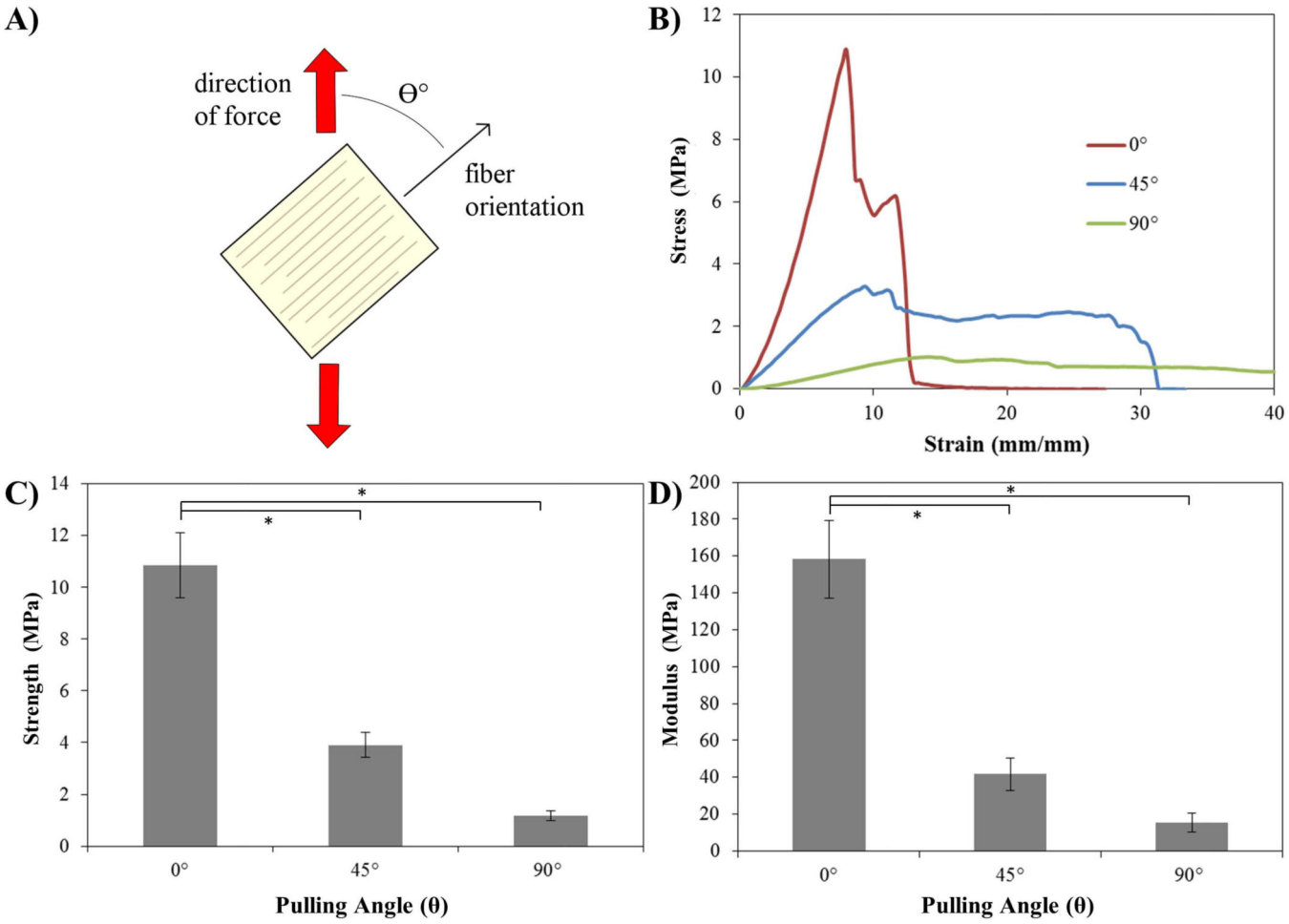

Fig. 5.

A) Schematic illustrating the nature of the uniaxial tensile test, where force is applied vertically (red arrows) and the tendon section samples are tested with fiber alignment in various directions. The samples were tested at angles (θ) of 0, 45 and 90°. All samples were 10 layers of 50μm each, crosslinked with glutaraldehyde in excess (5% for 30min). **B)** Representative stress-strain curves for samples tested at the various orientations. **C)** Graph illustrating the ultimate tensile strength of the samples tested in uniaxial tension at 0, 45 and 90°. **D)** Graph showing the elastic modulus as determined by linear regression of the samples tested at 0, 45 and 90°. Statistical differences marked with * ($p>0.05$), (n=4) for all samples. Strength and moduli values are given in Supplementary Fig. 1

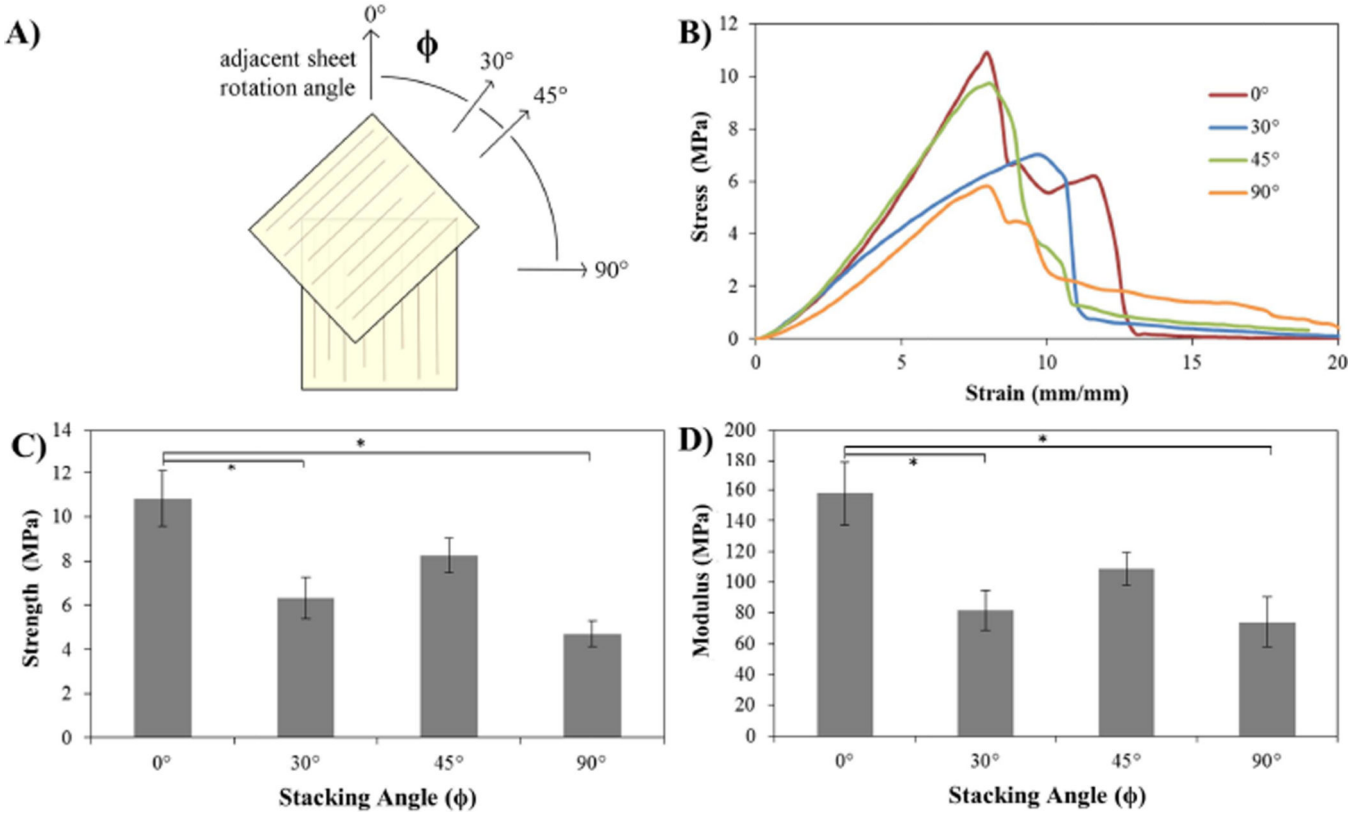

Fig. 6.

A) Schematic illustrating the stacking process. A single 50μm-thick section is placed at the 0° orientation and subsequent sections are stacked on top, rotated by either 0° (all aligned), 30°, 45° or 90° for a total of 12 layers. Each sample consisted of only one rotation angle and were subsequently crosslinked with glutaraldehyde (5%, 30min). The load during testing was applied in the direction of the first sheet. **B)** Representative stress-strain curves for samples tested at with the various rotation angles under uniaxial tension. **C)** Graph illustrating the ultimate tensile strength of the samples tested. **D)** Graph showing the elastic modulus as determined by linear regression of the samples tested at varying rotation angles. Statistical differences marked with * ($p>0.05$), ($n=4$) for all samples. Strength and moduli values are given in Supplementary Fig. 1